



## Article

# Synthesis of Silver Nanoparticles Using *Odontosoria chinensis* (L.) J. Sm. and Evaluation of their Biological Potentials

Marimuthu alias Antony samy Johnson <sup>1</sup>, Thangaiah Shibila<sup>1</sup>, Santhanam Amutha <sup>2</sup>, Irwin R.A. Menezes <sup>3</sup>, José G.M. da Costa <sup>3</sup>, Nadghia F. L. Sampaio <sup>3</sup> and Henrique D.M. Coutinho <sup>3,\*</sup>

<sup>1</sup> Centre for Plant Biotechnology, Department of Botany, St. Xavier's College (Autonomous), Palayamkottai, Tamil Nadu- 627 002, India; ptcjohnson@gmail.com (J.M.A.); anletshibila@gmail.com (T.S.)

<sup>2</sup> National Centre for Nanoscience and Nanotechnology, University of Madras, Chennai, Tamil Nadu 600025, India; amutha1994santhanam@gmail.com

<sup>3</sup> Department of Biological Chemistry, Centre of Biological Science and Health, Regional University of Cariri—URCA, 63105-000, Crato—CE, Brazil; galberto.martins@gmail.com (J.G.M.C.); nadghia.fl@gmail.com (N.F.L.S.)

\* Correspondence: hdmcoutinho@gmail.com; Tel.: +55(88)31021212; Fax: +55(88)-31021291

Received: 14 March 2020; Accepted: 7 April 2020; Published: 13 April 2020

**Abstract:** The present study was aimed to synthesize silver nanoparticles (AgNPs) from the aqueous extracts of *Odontosoria chinensis* (L.) J. Sm. and the synthesized AgNPs were examined for their biopotentials. The *Odontosoria chinensis* extracts were added to 1 mM AgNO<sub>3</sub> solution with different ratios viz., 0.5: 9.5, 1:9, 1.5: 8.5 and 2: 8 ratios for the reduction of Ag ions. After reduction, the AgNPs of *Odontosoria chinensis* were analyzed spectroscopically for further confirmation. The synthesized AgNPs of *Odontosoria chinensis* were characterized by pH, ultra violet–visible spectroscopy (UV-Vis), Fourier transform–infra red spectroscopy (FT-IR), scanning electron microscopy-energy dispersive X-ray analysis (SEM-EDAX) and X-Ray diffraction (XRD). The time taken for the complete reduction of Silver (Ag) in solution to nanoparticle was 10 min. The *O. chinensis* aqueous extracts mediated silver nanoparticles showed a broad peak with distinct absorption at around 400–420 nm and confirmed the silver nanoparticle formation. FT-IR results also confirmed the existence of organic materials in the silver nanoparticles of *O. chinensis*. The EDX spectra of AgNPs of *O. chinensis* revealed the occurrence of a strong Ag peak. The synthesis of AgNPs of *O. chinensis* was confirmed with the existence of a peak at 46.228°. The toxic potential of AgNPs of *O. chinensis* showed varied percentage mortality with the LC<sub>50</sub> values of 134.68 µL/50 mL and 76.5 µL/50 mL, respectively. The anti-inflammatory and anti-diabetic activities of aqueous and AgNPs of *O. chinensis* were statistically significant at  $p < 0.05$  level. Conclusion: The results demonstrated the toxicity, anti-diabetic and anti-inflammatory potential of the studied AgNPs. The synthesized nanoparticles of *Odontosoria chinensis* could be tested as an alternative to anticancer, anti-diabetic and anti-inflammatory drugs.

**Keywords:** anti-diabetic; anti-inflammatory; cytotoxic; silver nanoparticles; *Odontosoria chinensis*

## 1. Introduction

*Odontosoria chinensis* (L.) J. Sm. (Syn. *Trichomanes chinensis* L. and *Sphenomeris chinensis* (L.) Maxon) belongs to the family Lindsaeaceae and is a terrestrial herb found at higher altitudes [1]. The plant is used in the treatment of chronic enteritis [2,3]. Toji [4] identified the existence of flavonoids, phenols and steroids in the acetone and methanolic extracts of *Odontosoria chinensis*. In

addition, Toji [4] also observed the antibacterial activity of *Odontosoria chinensis* acetone extracts against *Pseudomonas aeruginosa* and *Staphylococcus aureus*. Methanolic and ethyl acetate extracts fraction showed significant antioxidant activities as well as antimicrobial activity against *Escherichia coli*. Two major secondary metabolites 3,4-dihydroxybenzoic acid and 3,4-dihydroxybenzaldehyde were isolated from *T. chinensis* leave, stem and root methanolic extracts [5]. Four aromatic compounds viz., 3,4 dihydroxybenzoic acid, 3,4-dihydroxybenzaldehyde, 4-hydroxy-3, 5-dimethoxybenzoic acid and 4-hydroxy-3-methoxy benzoic acid were isolated from *T. chinensis*. Al-Mekhlafi [6] studied the cytotoxic and acetylcholinesterase inhibitory activities of *Odontosoria chinensis* crude fractions. The whole plants of *Odontosoria chinensis* was used to treat itches [7].

Nowadays, silver nanoparticles have gained tremendous popularity at the global level in the field of agriculture, medicine, sensor, and pharmaceutical industries. Generally, two methods are used for the synthesis of silver nanoparticles viz., biological and chemical. Due to negative impacts on the ecosystem, time consumption and production cost, the chemical methods are not popularized [8]. On the other hand, biosynthesis of silver nanoparticles has attained its own importance due to time consumption for synthesis, and being economically cheap and more eco-friendly. For the last two decades, many researchers focused their attention to synthesize silver nanoparticles using natural products as the source [9–16]. With reference to pteridophytes, only very few reports are available for the green synthesis of AgNPs [17–19]. However, there is no report on *Odontosoria chinensis* (L.) J. Sm. mediated silver nanoparticle synthesis. Hence, the present study aimed to synthesize AgNPs from the aqueous extracts of *Odontosoria chinensis* (L.) J. Sm. and examine their anti-inflammatory, anti-diabetic and toxic effects.

## 2. Materials and Methods

Healthy and disease-free matured sporophytes without spores of *Odontosoria chinensis* (L.) J. Sm. (Indigenous to Hawaii, Phillipines and other parts of the tropics) were collected from Kodaikanal Botanical Garden, Eetipallam, Kodaikanal, Tamil Nadu, India. The collected sporophytes were washed in running tap water to remove the unwanted debris materials. The plant materials were dried and the excess water was removed using blotting paper.

A total of 10 g of matured sporophytes of *O. chinensis* without spores were cut into small pieces and boiled with 100 mL of distilled water for 30 min. After 30 min, the aqueous extracts were filtered using Whatman No. 1 filter paper. The filtered extracts were centrifuged at 3000 rpm for 10 min. The supernatants were collected and used for synthesis of AgNPs and further studies [16]. Qualitative analysis of the aqueous extracts was carried out according to the standard method described by Harborne [20]. The effects of AgNO<sub>3</sub> concentration (1mM–6mM), different time intervals for the reduction and various temperatures (30–90 °C) on the synthesis of AgNPs of *Odontosoria chinensis* were studied.

The *Odontosoria chinensis* extracts were added to 1 mM AgNO<sub>3</sub> solution with different ratio viz., 0.5: 9.5, 1:9, 1.5: 8.5 and 2: 8 ratios for the reduction of Ag ions. After reduction, the AgNPs of *Odontosoria chinensis* were analyzed spectroscopically for further confirmation. The reduction of pure Ag ions was monitored by measuring the ultra violet–visible spectroscopy (UV-Vis) spectrum of the solution at 400–900 nm using a Shimadzu spectrophotometer and the characteristic peaks were detected. The AgNPs and *Odontosoria chinensis* aqueous extracts were pelletized separately in IR-grade KBr (Hi Media, Mumbai, India). FT-IR (Fourier-transform infrared spectroscopy) analysis was performed using a Perkin Elmer Spectrophotometer system, USA over a frequency range 400–4000 cm<sup>-1</sup>, which was used to detect the characteristic peaks. Each and every analysis was repeated twice for the confirmation of the spectrum. The synthesized AgNPs of *Odontosoria chinensis* were characterized by pH and X-Ray Diffraction (XRD). Morphology and size of AgNPs were investigated by the FESEM (FEI-TECHNAI G2, Japan) the resolution was 1.0 nm/15 KV (1.6 nm/1 KV).

### 2.1. Toxicity Analysis

The toxicity of synthesized silver nanoparticles of *Odontosoria chinensis* was determined using *Artemia salina* (naupli) as the experimental animal [21]. Aqueous extracts and nanosolutions of *Odontosoria chinensis* AgNPs were taken in different concentrations (50, 100, 150, 200 and 250 µL/50 mL) and distilled water was used as the control. For each and every experimental concentration, 10 naupli were employed. After 24 h, the mortality of the naupli was observed. Each and every experiment was repeated thrice with five replicates. LC<sub>50</sub> at 95% confidence limit, LCL – Lower Confidence Limit and UCL – Upper Confidence Limit were calculated. The plumbagin was used as standard to estimate the toxicity.

## 2.2. Anti-Diabetic Activity

The aqueous and silver nanoparticles of *Odontosoria chinensis* were tested for its serum amylase inhibitory activity by the Yukihiro method [22]. Three test tubes were taken and labeled as blank (B), test (T) and control (C). Then, 2.5 mL of phosphate buffer with pH 6.8 was added to each tube. The substrate starch (1 mL) and sodium chloride were added to all the prepared aliquots. The test tubes were incubated at 37 °C for 10 min. After incubation, 0.5 mL of aqueous extract of *O. chinensis* was added and 0.2 mL of the enzyme (serum, amylase, pancreatic amylase, α-amylase from fermented barley) was added to the test tube. The contents of the test tube were mixed well and incubated at 37 °C for 10 min. After incubation, 0.5 mL of 2N NaOH was added to the test tube (T) and (C), 0.2 mL of enzymes was added to the control (C), 5.7 mL of distilled water alone served as the blank (B), and 0.2 mL of dinitrosalicylic acid was added to all the test tubes (T and C). The contents were mixed well and kept in a boiling water bath for 15 min. The standard acarbose was employed as a positive control. The intensity of reddish orange color was read at 540 nm. The percentage of inhibitory action was calculated using the following formula.

$$\text{Percentage inhibition} = \frac{\text{Optical Density (O.D) of control} - \text{O.D of test}}{\text{O.D of control}} \times 100 \quad (1)$$

## 2.3. Anti-Inflammatory Activity using Membrane stabilization Assay

### 2.3.1. Preparation of Red Blood Cells (RBCs) suspension

The blood was collected from a healthy human volunteer who had not taken any NSAIDs (non steroidal anti-inflammatory drugs) for 2 weeks prior to the experiment and transferred to the centrifuge tubes and centrifuged at 3000 rpm for 10 min. The tubes were washed thrice with equal volume of normal saline. The volume of blood was measured and reconstituted as 10% v/v suspension with normal saline [23,24].

### 2.3.2. Heat Induced Haemolysis

The reaction mixture (2 mL) includes 1 mL of different concentrations of aqueous and silver nanoparticles of *Odontosoria chinensis* (50, 100, 200 and 250 µg/mL) and 1 mL of 10% RBCs suspension. For the negative control, the saline was added instead of plant extracts. Aspirin was employed as a positive control. The reaction mixtures were incubated in a water bath at 56 °C for 30 min. After incubation, the tubes were kept in running tap water. The reaction mixtures were centrifuged at 3000 rpm for 5 min and the absorbance of the supernatants was measured at 560 nm [25]. The experiment was performed in triplicate for all the test samples. As a standard, 100 µg/mL of Indomethacin was used.

The percentage inhibition of haemolysis was calculated as follows:

$$\text{Percentage inhibition} = \frac{\text{Abs control} - \text{Abs sample}}{\text{Abs control}} \times 100 \quad (2)$$

Statistical analysis was performed using SPSS 21 software. Analysis of variance and pair wise Pearson and Spearmen correlation tests were performed. The *p* value < 0.05 was considered as significant.

### 3. Results

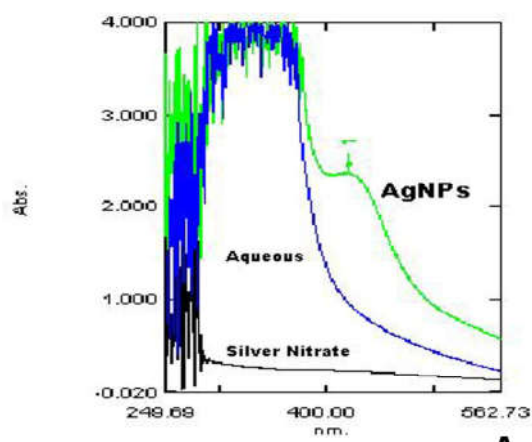
#### 3.1. Synthesis of *O. chinensis* AgNPs

Among the various ionic concentrations of AgNO<sub>3</sub> tested, the stable nanoparticle of *Odontosoria chinensis* was obtained at 1 mM (1:9 ratios) concentration of AgNO<sub>3</sub>. Among the various temperatures examined for the synthesis of silver nanoparticles of *O. chinensis*, the nanoparticle synthesized at 40 °C showed small size of nanoparticles (22.3–48.2 nm). The silver nanoparticles synthesised above 40 °C demonstrated the occurrence of agglomeration of AgNPs. Green synthesized AgNPs of *O. chinensis* were stable for 6 months without shifting the surface plasmon absorbance band and free from microbial contamination. AgNO<sub>3</sub> solution mixing with aqueous extracts of *O. chinensis* showed that the color of the solution changed from colorless or pale yellow to a yellowish brown color and indicated the presence of AgNPs. The time taken for the complete reduction of Ag in solution to nanoparticle was 10 min. After 2 h of incubation, no further increase in color intensity was found in the AgNPs of *O. chinensis*, indicating the complete reduction of silver ions. The pH of the AgNO<sub>3</sub> solution was also changed from 3.87 to 4.56 when the AgNO<sub>3</sub> solution was mixed with *O. chinensis* aqueous extracts. The change of pH suggested the capping between Ag and *O. chinensis* aqueous extracts.

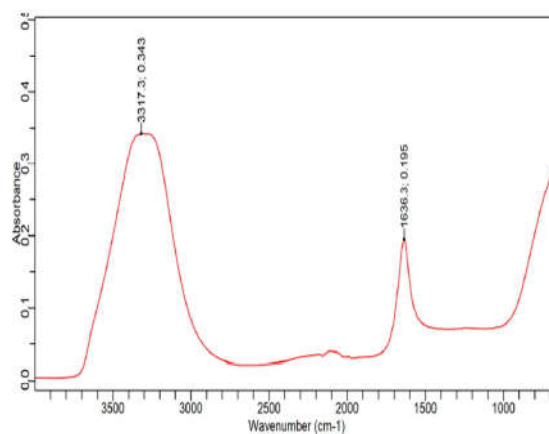
#### 3.2. Spectroscopic Analysis of *O. chinensis* AgNPs

The absorption peak (SPR) was observed in the visible range at 405 nm. UV-Vis spectra of *O. chinensis* aqueous extracts failed to display an absorption in the range of 400–800 nm but the *O. chinensis* aqueous extracts mediated silver nanoparticles showed a broad peak with distinct absorption at around 400–420 nm and confirmed the silver nanoparticle formation (Figure 1 A). In addition, the silver nanoparticles of *O. chinensis* displayed a peak at 660 nm and confirmed the existence of some phytoconstituents.

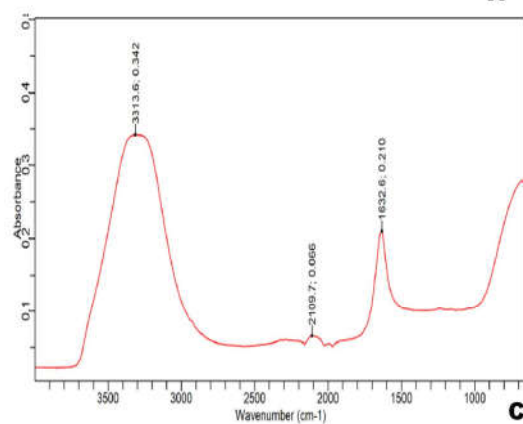
In the present study, FT-IR was used to identify the chemical composition of surface, local molecular environment, reducing and capping agents of synthesized silver nanoparticles of *O. chinensis*. The results of FT-IR analysis of *O. chinensis* silver nanoparticles showed different stretches of bonds with varied peaks (Figures 1B and 1C). The peak, 3317.3 cm<sup>-1</sup>, was assigned to O – H stretch in the reducing agent (phenol), 2109.7 cm<sup>-1</sup> to the CH stretch in alkane and 1632.6 cm<sup>-1</sup> to C–C stretch (in-ring) from carbonyl stretch in aromatics. Fourier transforms infra radiation (FTIR) spectroscopic peak profiles were used to confirm the presence of carboxylic acid on the green synthesized silver nanoparticles. This study results also confirmed the existence of organic materials in the silver nanoparticles of *O. chinensis*. These FT-IR spectroscopic study results confirmed that *O. chinensis* aqueous extracts possess the capacity to perform dual functions of reduction and stabilization of silver nanoparticles.



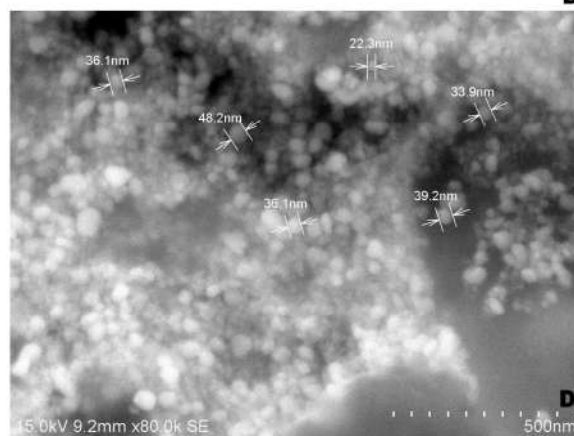
**A**



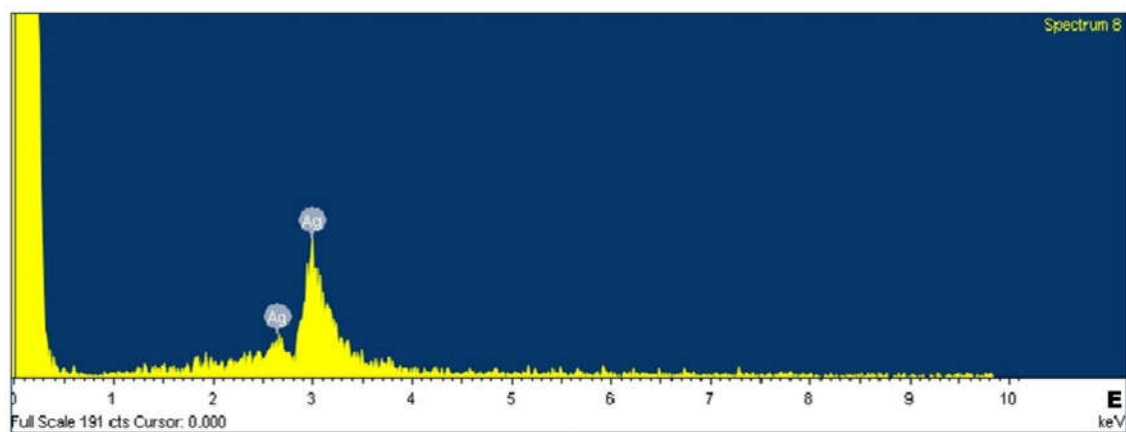
**B**



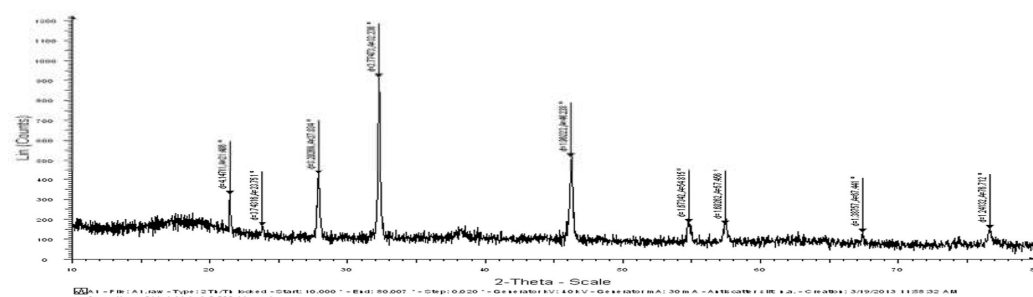
**C**



D



**E**

**F**

**Figure 1.** Biosynthesis of silver nanoparticles (AgNPs) of *O. chinensis*; UV-Vis spectrum of aqueous, silver nitrate and silver nanoparticles of *O. chinensis* (A); FT-IR spectrum of *O. chinensis* aqueous extracts (B); Fourier-transform infrared (FT-IR) spectrum of silver nanoparticles of *O. chinensis* (C); scanning electron microscopy (SEM) photograph of silver nanoparticles of *O. chinensis* (D); energy dispersive X-ray analysis (EDAX) spectrum of *O. chinensis* silver nanoparticles (E); X-Ray diffraction (XRD) pattern of *O. chinensis* silver nanoparticles (F)

### 3.3. SEM-EDAX Analysis of *O. chinensis* AgNPs

The morphological characters of synthesized AgNPs of *O. chinensis* were determined using a scanning electron microscope (Figure 1D). The size of *O. chinensis* AgNP was observed in the range of 22.3–48.2 nm. The average size of the nanoparticle is  $35.97 \pm 8.38$  nm. However, further observations with higher magnification reveal that these crowded AgNPs are groups of smaller nanoparticles that exhibit good uniformity. The spherical and oval shaped AgNPs of *O. chinensis* was observed (Figure 1D). The SEM-EDAX confirmed the existence of silver in the AgNPs of *O. chinensis* (Figure 1E)

### 3.4. XRD Analysis of *O. chinensis* AgNPs

The XRD spectra of AgNPs of *O. chinensis* revealed the occurrence of a strong Ag peak. The XRD pattern of *O. chinensis* nanoparticles illustrated 9 peaks at  $21.406^\circ$ ,  $23.751^\circ$ ,  $27.834^\circ$ ,  $32.236^\circ$ ,  $46.228^\circ$ ,  $54.815^\circ$ ,  $57.456^\circ$ ,  $67.441^\circ$  and  $76.712^\circ$  (Figure 1F). The synthesis of AgNP's of *O. chinensis* confirmed with the existence of a peak at  $46.228^\circ$ .

### 3.5. Biopotency of *O. chinensis* AgNPs

The toxic potential of the aqueous extracts and AgNPs of *O. chinensis* showed varied percentage mortality with the  $LC_{50}$  values of  $134.68 \mu\text{l} / 50 \text{ mL} = 2.69 \mu\text{l} / \text{ml}$  and  $76.48 \mu\text{l} / 50 \text{ mL} = 1.53 \mu\text{L/mL}$ , respectively. A dose dependent toxicity was observed in AgNPs of *O. chinensis* (Figure 2). The standard plumbagin showed 100% mortality of brine shrimp nauplii at  $0.046 \text{ mg/mL}$ . Similar to toxicity, the dose dependent anti-inflammatory and anti-diabetic activities were observed in the aqueous and AgNPs' of *O. chinensis* (Figures 3 and 4). The AgNPs of *O. chinensis* showed to be more anti-inflammatory and inhibited the specific enzymes responsible for anti-diabetic activities than the aqueous extracts of *O. chinensis* (Figures 3 and 4). The anti-inflammatory and anti-diabetic activities of aqueous and AgNPs' of *O. chinensis* were statistically significant at  $p < 0.05$  level. The standard indomethacin ( $100 \mu\text{g/mL}$ ) showed 71.43% inhibition. The standard acarbose  $500 \mu\text{g/mL}$  showed 78% activity. A strong positive correlation was observed with various concentrations of aqueous extracts and anti-inflammatory activity of *O. chinensis* with the correlation coefficient  $R = 0.972$  and silver nanoparticles of *O. chinensis* with the correlation coefficient  $R = 0.965$ . The correlation was significant at the 0.05 level (2-tailed). A strong positive correlation was observed with various concentrations of aqueous extracts and anti-diabetic activity of *O. chinensis* with the correlation coefficient  $R = 0.983$  and silver nanoparticles of *O. chinensis* with the correlation coefficient  $R = 0.78$ . The correlation was significant at the 0.05 level (2-tailed).

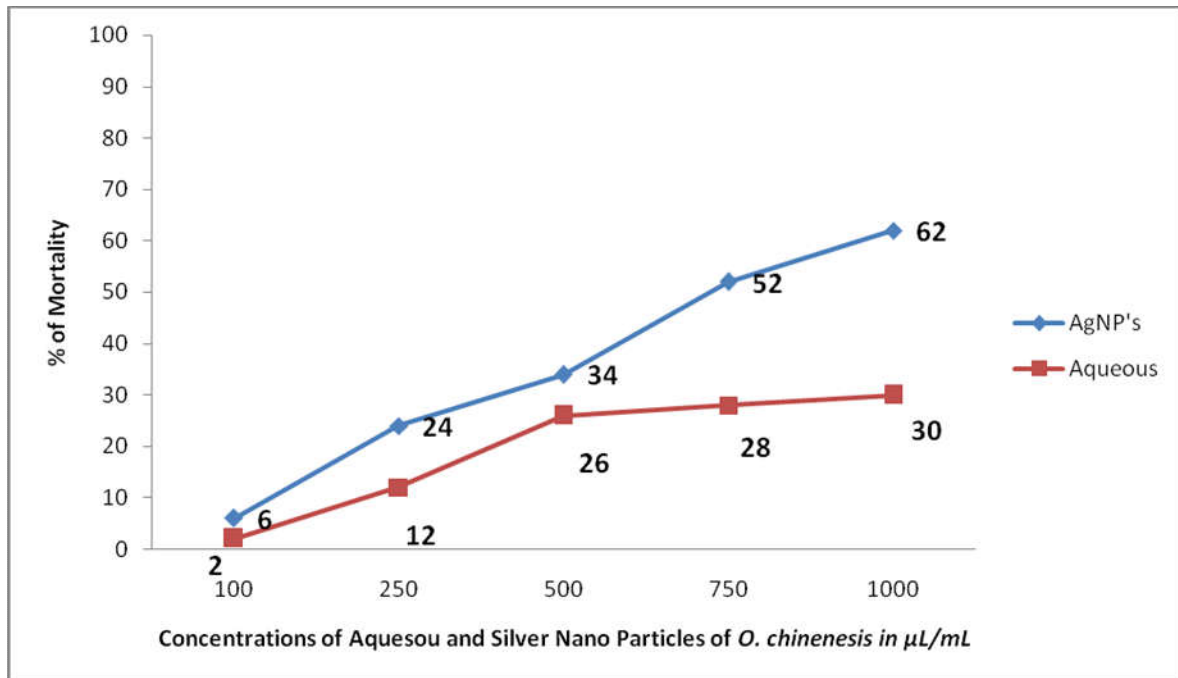


**Figure 2.** Toxic potential of the aqueous extracts and AgNPs of *O. chinensis*.

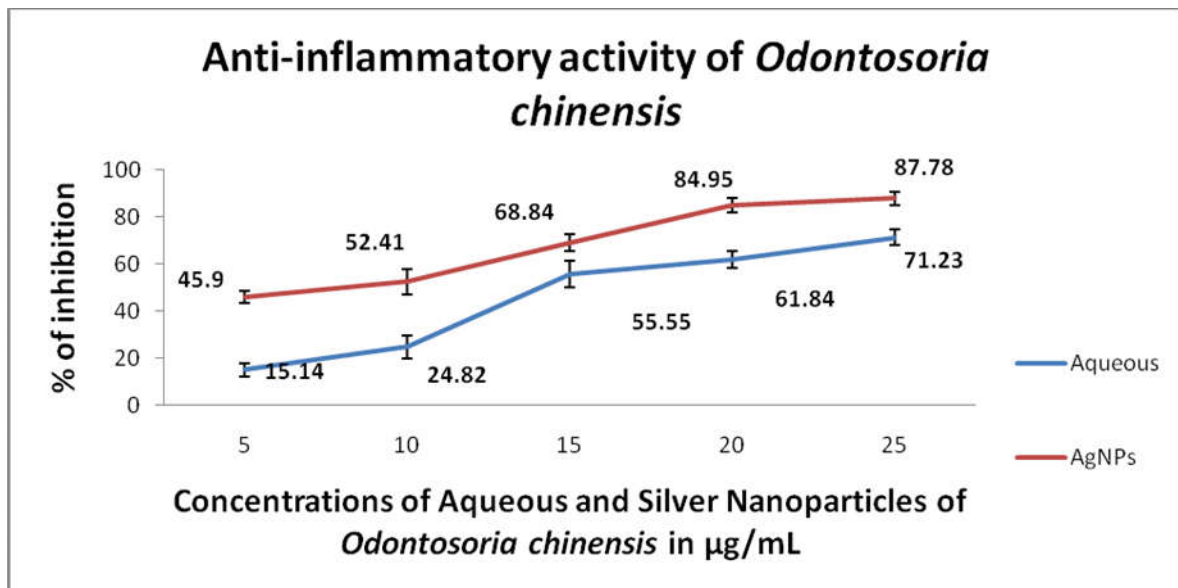


**Figure 3.** Anti-inflammatory activity of the aqueous extracts and AgNPs of *O. chinensis*.

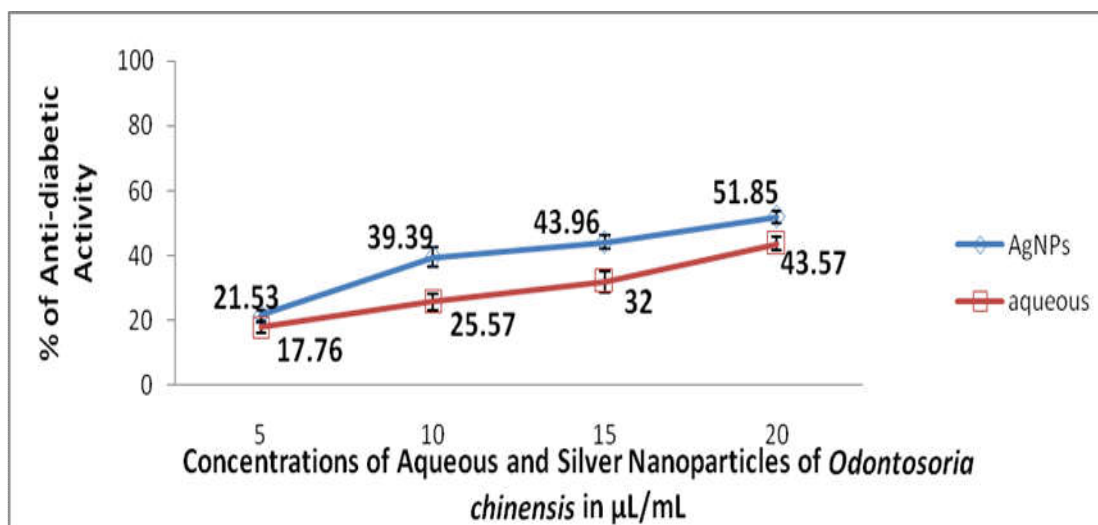


Figure 4. Anti-diabetic activity of the aqueous extracts and AgNPs of *O. chinensis*.

#### 4. Discussion

Generally, 1mM AgNO<sub>3</sub> (1:9 ratio) was employed for the synthesis of silver nanoparticles from Pteridophytes [16–19]. The nanoparticles were stable up to six months without any contamination. In the present study, 1 mM of silver nitrate also produced good nanoparticles of *O. chinensis*. Similar results were observed in *Cyathea nilgirensis* in our previous research, carried out in our lab. Among the various ratios of *O. chinensis* extracts with 1 mM AgNO<sub>3</sub> screened, the 1:10 ratio was optimized for silver nanoparticle synthesis. Bhor et al. [24], Nalwade et al. [18], Sant et al. [26] and Johnson et al. [16] employed 1:10 silver nitrate and plant extracts ratio for the synthesis of silver nanoparticles from *Nephrolepis exaltata*, *Cheilanthes farinosa*, *Adiantum phillippense* and *Cyathea nilgirensis*. In the present study, 10 mL of *O. chinensis* and 90 mL of 1mM silver nitrate also yielded good nanoparticles. Commonly, the UV-Vis spectroscopy was employed to confirm the nanoparticle formation [27]. Feldheim and Foss [28] suggested the light wave length ranges i.e., 300 to 800 nm for characterizing various nanoparticles. Huang et al. [29] further confirmed the spectroscopic measurement for nanoparticles at 400–450 nm. Shivakumar and Vidyasagar [30] and Christopher et al. [31] observed a characteristic peak for silver nanoparticle of at 420 nm for *Annona reticulata* and *Aegle marmelos*, respectively. In the present study, a characteristic peak was also observed at 405 nm for the silver nanoparticles of *O. chinensis*. These UV-Vis analysis results suggest that the phytoconstituents that occurred in the aqueous extracts of *O. chinensis* may be responsible for the reduction. Preliminary phytochemical analysis of *O. chinensis* aqueous extracts confirmed the presence of terpenoids, tannins, coumarins, phenolics and steroids. These metabolites are responsible for the bio-reduction of AgNPs. Earlier studies indicated that the reduction of silver ions and stability of AgNPs are due to the occurrence of phytoconstituents or metabolites present in the source extracts [32]. To probe the chemical composition of the surface and the local molecular environment, reducing and capping agents of the silver nanoparticles, FT-IR spectroscopy was employed [16]. In the present study, reduction and capping of the silver nanoparticles of *Odontosoria chinensis* was also confirmed by the FT-IR analysis.

Brine shrimp bioassay was employed to determine the different pharmacological properties of the plant extracts [33]. In this study, toxic effects of *Odontosoria chinensis* nanoparticles towards shrimp's larvae were studied. A dose dependent toxicity was observed in AgNPs of *O. chinensis*. The AgNPs of *O. chinensis* showed more toxic activities than the aqueous extracts of *O. Chinensis*. The toxic effects of *O. chinensis* nanoparticles can be correlated with anticancer activity of the *O. chinensis* nanoparticles. The results of the present study directly coincide with Johnson et al.'s [16] observation on AgNPs of *C. nilgirensis*. The results of the present study suggested that *O. chinensis* AgNPs treatment against *Artemia salina* inhibited the viability. In control experiments, it was clearly

indicated that all the concentrations of aqueous and AgNPs extracts did not induce any lethal effect on *A. salina*. We observed the morphological changes, which disrupted and affected movement and feeding, which resulted mainly in decreased swimming ability. Intestinal enlargement, loss of antennae and deformation of antennae occurred in *A. salina* exposed to *O. chinensis* aqueous extract and AgNPs of *O. chinensis*. However, we failed to observe the significant changes in *A. salina* cultured in the control (saline water). From the results, the percentage of mortality rate was extensively increased, which corresponds to the concentration of aqueous and *O. chinensis* AgNPs. The exposure of silver nanoparticles of *O. chinensis* may generate the reactive oxygen species (ROS) that may cause cytotoxicity [34]. The synthesized nanoparticles of *Odontosoria chinensis* could be an alternative source of anticancer drugs [35].

Preliminary phytochemical analysis of *O. chinensis* aqueous extracts confirmed the presence of terpenoids, tannins, coumarins, phenolics and steroids. The FT-IR analysis results confirmed the occurrence of polyphenols/phenols in the silver nanoparticles of *O. chinensis*. The occurrence of tannins, phenolics and terpenoids are responsible for the anti-inflammatory and anti-diabetic activities of the silver nanoparticles and aqueous extracts of *O. chinensis*. The tannins prevent hyperglycemia by inhibiting aldose reductase in vitro and induced lens pacification on organ culture. Tannins also inhibit sorbitol formation in the lens, and might counter the polyol pathway induced oxidative stress. Suryanarayana [36] reported the anti-diabetic properties of tannoids. The high phenolic content of the aqueous extracts of the *O. chinensis* support the anti-amylase activity. The phenolic substances have the ability to interact with and/or inhibit proteins/enzymes [37]. The Spearman and Pearson correlation results clearly explained the dose dependent protection of the studied aqueous and AgNPs, with 0.982 of *O. chinensis*, and correlation was significant at the 0.01 level (2-tailed). Similar to our observation, Shaik et al. [38] also observed the highest percentage of antibacterial activity in the silver nanoparticles of *Origanum vulgare* compared with aqueous extracts of *Origanum vulgare*. The *Origanum vulgare* extract failed to display any microbicidal activity up to 300 µg, but the AgNPs prepared from *Origanum vulgare* displayed microbicidal activity. Similarly, the viability of tumor cells treated with AgNPs were greatly affected ( $88 \pm 4.44\%$  cell death) compared with untreated cells (2% cell death) after 24 h of incubation [11].

## 5. Conclusion

The results of the present study clearly explain the toxicity, anti-diabetic and anti-inflammatory potentials of the studied silver nanoparticles of *Odontosoria chinensis*. The synthesized nanoparticles of *Odontosoria chinensis* could be tested as an alternative source of anticancer, anti-diabetic and anti-inflammatory drugs.

**Author Contributions:** Johnson, Amutha, Countinho—Designing the experiemnt, Supervision, manuscript writing, Shibila, Menezes, Costa, Sampaio—execution of the experiemnt. All authors have read and agreed to the published version of the manuscript.

**Funding:** This research received no external funding.

**Conflicts of Interest:** The authors declare no conflict of interest

## References

1. Souza, R.K.D.; Da Silva, M.A.P.; De Menezes, I.R.A.; Ribeiro, D.A.; Bezerra, L.R.; Souza, M.M.D.A. Ethnopharmacology of medicinal plants of carrasco, northeastern Brazil. *J. Ethnopharmacol.* **2014**, *157*, 99–104, doi:10.1016/j.jep.2014.09.001.
2. Easa, P.S. Biodiversity documentation for Kerala Part 5: Pteridophytes. In *Peechi: Kerala Forest Research Institute Kerala KRFRI Hand Book*; 2003; KRFRI, Kerala, India, Volume 17, p. 36.
3. Nayar, B.K. Medicinal ferns of India. National Botanic Gardens Lucknow India. *Bulletin* **1959**, *29*, 1–29.
4. Vasudeva, S.M. Economic importance of pteridophytes. *Indian Fern. J.* **1999**, *16*, 130–152.
5. Toji, T. Preliminary Antibacterial and Phytochemical Evaluation of *Odontosoria chinensis* (L.). *J. Sm. J. Pharmacogn. Herb. Formul.* **2011**, *1*, 26–30.

6. Syafni, N.; Putra, D.P.; Arbain, D. 3,4-DIHYDROXYBENZOIC ACID AND 3,4-DIHYDROXYBENZALDEHYDE FROM THE FERN *Trichomanes chinense* L.; ISOLATION, ANTIMICROBIAL AND ANTIOXIDANT PROPERTIES. *Indones. J. Chem.* **2012**, *12*, 273–278.
7. Al-Mekhlafi, N.A. Phytochemical, Cytotoxic and Acetylcholinesterase inhibition in Kacip Fatimah (*Labisia pumila* (Blume), Fern Vill), Penarahan (*Hosfieldia superba* (HK.F.& Th.) Warb) and Paku Layar (*Odontosoria chinensis* (L) J. Sm.) Extracts. Ph.D. Thesis, University Patra Malaysia, Malaysia, 2011; Volume 8.
8. Iravani, S.; Korbekandi, H.; Mirmohammadi, S.; Zolfaghari, B. Synthesis of silver nanoparticles: chemical, physical and biological methods. *Res. Pharm. Sci.* **2015**, *9*, 385–406.
9. Asha, K.S.; Johnson, M.; Chandra, P.K.; Shibila, T.; Revathy, I. Extracellular Synthesis of Silver Nanoparticles from A Marine Alga, *Sargassum polycystum* C. Agardh and Their Bio-potentials. *World J. Pharm. Pharm. Sci.* **2016**, *4*, 1388–1400.
10. Narayani, M.; Johnson, M. Novel synthesis of silver nanopetides using protein extracts of *Selaginella intermedia* (Bl.) String. In *Medicinal Plants: Phytochemistry, Pharmacology and Therapeutics*; Gupta, V.K., Singh, G.D., Singh, S., Kaul, A., Ed.; Daya Publishing House: New Delhi, India, 2015; pp. 489–497.
11. Sulaiman, G.M.; Hussien, H.T.; Saleem, M.M. Biosynthesis of silver nanoparticles synthesized by *Aspergillus flavus* and their antioxidant, antimicrobial and cytotoxicity properties. *Bull. Mater. Sci.* **2015**, *38*, 639–644.
12. Al-Shmgani, H.S.A.; Mohammed, W.H.; Sulaiman, G.M.; Saadoon, A.H. Biosynthesis of silver nanoparticles from *Catharanthus roseus* leaf extract and assessing their antioxidant, antimicrobial, and wound-healing activities. *Artif. Cells Nanomedicine, Biotechnol.* **2017**, *45*, 1234–1240, doi:10.1080/21691401.2016.1220950.
13. Ismail, R.A.; Sulaiman, G.M.; Mohsin, M.H.; Saadoon, A.H. Preparation of silver iodide nanoparticles using laser ablation in liquid for antibacterial applications. *IET Nanobiotechnology* **2018**, *12*, 781, doi:10.1049/iet-nbt.2017.0231.
14. Taha, Z.K.; Hawar, S.N.; Sulaiman, G.M. Extracellular biosynthesis of silver nanoparticles from *Penicillium italicum* and its antioxidant, antimicrobial and cytotoxicity activities. *Biotechnol. Lett.* **2019**, *41*, 899–914, doi:10.1007/s10529-019-02699-x.
15. Chandra Kala, P.; Johnson, M.; Shibila, T.; Revathy, I. Synthesis and Characterization of Cytotoxic Silver Nanoparticles Using Marine Brown Seaweed *Sargassum johnstonii* Setchell & N.L.Gardner. *World J. Pharm. Res.* **2015**, *4*, 1545–1555.
16. Antonyamy, M.J.A.; Santhanam, A.; Thangaiah, S.; Narayanan, J.; Johnson, M.; Amutha, S.; Shibila, T.; Janakiraman, N. Green synthesis of silver nanoparticles using *Cyathea nilgirensis* Holttum and their cytotoxic and phytotoxic potentials. *Part. Sci. Technol.* **2017**, *36*, 578–582, doi:10.1080/02726351.2016.1278292.
17. Koteswaramma, J.K.; Varalaksmi, S. Biological synthesis of silver nanoparticle from aqueous extract of *Actinopterys radiata* and evaluation of their antimicrobial activity. *Int. J. Pharm. Bio. Sci.* **2017**, *8*, 121–125, doi:10.22376/ijpbs.2017.8.1.b121-125.
18. Nalwadea, A.R.; Badheb, M.N.; Pawalec, C.B.; Hinge, S.B. Rapid biosynthesis of silver nanoparticles using fern leaflet extract and evaluation of their antibacterial activity. *Int. J. Biol. Technol.* **2012**, *4*, 12–18.
19. Korbekandi, H.; Chitsazi, M.R.; Asghari, G.; Najafi, R.B.; Badii, A.; Iravani, S. Green biosynthesis of silver nanoparticles using *Azolla pinnata* whole plant hydroalcoholic extract. *Green Process. Synth.* **2014**, *3*, 365–373, doi:10.1515/gps-2014-0042.
20. Harborne, J.B. *Phytochemical Methods: A Guide to Modern Techniques of Plant Analysis*, 3rd ed.; Chapman Hall: New York, NY, USA, 1998.
21. McLaughlin, J.L.; Rogers, L.L. The use of biological assays to evaluate botanicals. *Drug Inf. J.* **1998**, *32*, 513–524, doi:10.1177/009286159803200223.
22. Yukihiko, H.; Miwa, H. The Inhibition of  $\alpha$  Amylase by Tea Polyphenols. *Agric. Biol. Chem.* **1990**, *54*, 1939–1945, doi:10.1080/00021369.1990.10870239.
23. Sakat, S.; Juvekar, A.R.; Gambhire, M.N. In vitro antioxidant and anti-inflammatory activity of methanol extract of *Oxalis corniculata* Linn. *Int. J. Pharma Pharmacol. Sci.* **2010**, *2*, 146–155.
24. Sadique, J.; Al-Rqobahs, W.A.; ElGindi, A.B.R. The bioactivity of certain medicinal plants on the stabilization of RBS membrane system. *Fitoterapia* **1989**, *60*, 525–532.

25. Bhor, G.; Maskare, S.; Hinge, S.; Singh, L.; Nalwade, A. Synthesis of Silver Nanoparticles Using Leaflet Extract of *Nephrolepis exaltata* L. and Evaluation Antibacterial Activity against Human and Plant Pathogenic Bacteria. *Asian J. Pharm. Technol. Innov.* **2014**, *2*, 23–31.
26. Sant, D.G.; Gujarathi, T.R.; Harne, S.R.; Ghosh, S.; Kitture, R.; Kale, S.; Chopade, B.A.; Pardesi, K.R. *Adiantum philippense* L. Frond Assisted Rapid Green Synthesis of Gold and Silver Nanoparticles. *J. Nanoparticles* **2013**, Article ID 182320, 9 pages. doi:10.1155/2013/182320.
27. Pal, S.; Tak, Y.K.; Song, J.M. Does the Antibacterial Activity of Silver Nanoparticles Depend on the Shape of the Nanoparticle? A Study of the Gram-Negative Bacterium *Escherichia coli*. *Appl. Environ. Microbiol.* **2007**, *73*, 1712–1720, doi:10.1128/AEM.02218-06.
28. Feldheim, D.L.; Foss, C.A. *Metal nanoparticles: Synthesis, Characterization, and Applications*; CRC Press: Boca Raton, FL, USA, 2002.
29. Huang, J.; Li, Q.; Sun, D.; Lu, Y.; Su, Y.; Yang, X.; Wang, H.; Wang, Y.; Shao, W.; He, N.; et al. Biosynthesis of silver and gold nanoparticles by novel sundried *Cinnamomum camphora* leaf. *Nanotechnol.* **2007**, *18*, 105104, doi:10.1088/0957-4484/18/10/105104.
30. Singh, P.S.; Manikrao, V.G. Biosynthesis, Characterization, and Antidermatophytic Activity of Silver Nanoparticles Using Raamphal Plant ( *Annona reticulata* ) Aqueous Leaves Extract. *Indian J. Mater. Sci.* **2014**, *2014*, 1–5, doi:10.1155/2014/412452.
31. Christopher, J.G.; Saswati, B.; EzilRani, P. Optimization of Parameters for Biosynthesis of Silver Nanoparticles Using Leaf Extract of *Aegle marmelos*. *Braz. Arch. Boil. Technol.* **2015**, *58*, 702–710, doi:10.1590/S1516-89132015050106.
32. Shankar, S.S.; Rai, A.; Ankamwar, B.; Singh, A.; Ahmad, A.; Sastry, M. Biological synthesis of triangular gold nanoprisms. *Nat. Mater.* **2004**, *3*, 482–488.
33. Hatano, T.; Edamatsu, R.; Hiramatsu, M.; Mori, A.; Fujita, Y.; Yasuhara, T.; Yoshida, T.; Okuda, T. Effects of the interaction of tannins with Co-existing substances. VI. Effects of tannins and related polyphenols on superoxide anion radical, and on 1,1-diphenyl-2-picrylhydrazyl radical. *Chem. Pharm. Bull.* **1989**, *37*, 2016–2021, doi:10.1248/cpb.37.2016.
34. Guo, D.; Zhao, Y.; Zhang, Y.; Wang, Q.; Huang, Z.; Ding, Q.; Guo, Z.; Zhou, X.; Zhu, L.; Gu, N. The cellular uptake and cytotoxic effect of silver nanoparticles on chronic myeloid leukemia cells. *J. Biomed. Nanotechnol.* **2014**, *10*, 669–678, doi:10.1166/jbn.2014.1625.
35. Ghareeb, M.A.; Hussein, A.H. Antioxidant and cytotoxic activities of *Tectona grandis* Linn. Leaves. *Int. J. Phytopharm.* **2014**, *5*, 143–157.
36. Suryanarayana, P.; Kumar, P.A.; Saraswat, M.; Petrash, M.; Reddy, G.B. Inhibition of aldose reductase by tannoid principles of *Embllica officinalis*: implications for the prevention of sugar cataract. *Mol. Vis.* **2004**, *10*, 1291–1297.
37. Rohn, S.; Rawel, H.; Kroll, J. Inhibitory Effects of Plant Phenols on the Activity of Selected Enzymes. *J. Agric. Food Chem.* **2002**, *50*, 3566–3571, doi:10.1021/jf011714b.
38. Shaik, M.R.; Khan, M.; Kuniyil, M.; Kuniyil, M.; Alkathlan, H.Z.; Siddiqui, M.R.H.; Shaik, J.P.; Ahamed, A.; Mahmood, A.; Khan, M.; et al. Plant-Extract-Assisted Green Synthesis of Silver Nanoparticles Using *Origanum vulgare* L. Extract and Their Microbicidal Activities. *Sustain.* **2018**, *10*, 913, doi:10.3390/su10040913.

